DOI: 10.1002/chem.200500471

Novel Luminescent Mixed-Metal Pt–Tl-Alkynyl-Based Complexes: The Role of the Alkynyl Substituent in Metallophilic and $\eta^2(\pi\cdots Tl)$-Bonding Interactions

Jesús R. Berenguer,[a] Juan Forniés,*[b] Belén Gil,[a] and Elena Lalinde*[a]

Abstract: A novel series of $[PtTl_2(C{\equiv}CR)_4]_n$ ($n=2$, R = 4-$CH_3C_6H_4$ (Tol) **1**, 1-naphthyl (Np) **2**; $n=\infty$, R = 4-$CF_3C_6H_4$ (Tol_F) **3**) complexes has been synthesized by neutralization reactions between the previously reported $[Pt(C{\equiv}CR)_4]^{2-}$ (R = Tol, Tol_F) or novel $(NBu_4)_2[Pt(C{\equiv}CNp)_4]$ platinum precursors and Tl^I ($TlNO_3$ or $TlPF_6$). The crystal structures of $[Pt_2Tl_4(C{\equiv}C\text{-}Tol)_8]\cdot 4$ acetone, **1**·4 acetone, $[Pt_2Tl_4(C{\equiv}CNp)_8]\cdot 3$ acetone·$^1/_3H_2O$, **2**·3 acetone·$^1/_3H_2O$ and $[\{PtTl_2(C{\equiv}CTol_F)_4\}(acetone)S]_\infty$ (S = acetone **3a**; dioxane **3b**) have been solved by X-ray diffraction studies. Interestingly, whereas in the tolyl (**1**) and naphthyl (**2**) derivatives, the thallium centers exhibit a bonding preference for the electron-rich alkyne entities to yield crystal lattices based on sandwich hexanuclear $[Pt_2Tl_4(C{\equiv}CR)_8]$ clusters (with additional Tl···acetone (**1**) or Tl···naphthyl (**2**) secondary interactions), in the $C_6H_4CF_3$ (Tol_F) derivatives **3a** and **3b** the basic Pt^{II} center forms two unsupported Pt–Tl bonds. As a consequence **3a** and **3b** form an extended columnar structure based on trimetallic slipped $PtTl_2(C{\equiv}CTol_F)_4$ units that are connected through secondary Tl···(η^2-acetylenic) interactions. The luminescent properties of these complexes, which in solution (blue; CH_2Cl_2 **1**,**2**; acetone **3**) are very different to those in solid state (orange), have been studied. Curiously, solid-state emission from **1** is dependent on the presence of acetone (green) and its crystallinity. On the other hand, while a powder sample of **3** is pale yellow and displays blue (457 nm) and orange (611 nm) emissions, the corresponding pellets (KBr, solid) of **3**, or the fine powder obtained by grinding, are orange and only exhibit a very intense orange emission (590 nm).

Keywords: acetylide · cluster compounds · columnar structure · luminescence · platinum · thallium

[a] Dr. J. R. Berenguer, B. Gil, Dr. E. Lalinde
Departamento de Química
Grupo de Síntesis Química de La Rioja, UA-C.S.I.C.
Universidad de La Rioja, 26006 Logroño (Spain)
Fax: (+34) 941-299-621
E-mail: elena.lalinde@dq.unirioja.es

[b] Prof. Dr. J. Forniés
Departamento de Química Inorgánica
Instituto de Ciencia de Materiales de Aragón
Universidad de Zaragoza-C.S.I.C., 50009 Zaragoza (Spain)
Fax: (+34) 976-761-187
E-mail: juan.fornies@posta.unizar.es

Supporting information for this article is available on the WWW under http://www.chemeurj.org/ or from the author. Expansions of the crystalline structures of **2**·3 acetone·$^1/_3H_20$ and **3b**, and coordination environments for the thallium atoms in the structure of **3b**. Absorption spectra of complexes **1**–**3**, together with those of the corresponding precursors, including the absorption spectra of complex **3** at different concentrations in a selected region (around 440 nm). Emission spectra of a crystalline sample of **1**·4 acetone in the solid state at different temperatures, as well as the emission spectra in the solid state of the dull yellow-orange solid obtained by elimination of acetone from **1**. Emission spectra of **3** at room temperature in pressed solid pellets.

Introduction

The search for supramolecular arrays is a productive area of research in materials chemistry.[1–5] Among these, one-dimensional extended systems are particularly interesting owing to their potentially useful chemical and photophysical properties.[6–8] In this field, increasing attention is currently being devoted to the construction of extended chains that are based on weak noncovalent closed-shell metal–metal bonding interactions.[9–24]

In particular, platinum-d^8 complexes have proven to be versatile building blocks for the formation of stacked linear-chain materials with short Pt···Pt contacts,[25–30] which are notably enhanced by strong-field and π-acidic ligands such as CN^- or CNR. Remarkable examples include the well-known simple, partially oxidized $[Pt(CN)_4]_n^{2n-}$ salts[31,32] and the double salts $[Pt(CNAr)_4][Pt(CN)_4]$ reported recently by Mann and co-workers,[33–35] which display vapochromic behavior. Considerable experimental work and theoretical calculations[11,36,37] seem to indicate that this type of metal–

metal contact is frequently reinforced by electrostatic components, as well as by charge-transfer-type dispersive contributions. In fact, such electrostatic attractions have been shown to be particularly strong with platinate(II) anions, as illustrated by the numerous examples of $Pt^{II}\rightarrow M$ dative-bond complexes (M = acid cation) presently known.[38–40] Following the report of the first luminescent and, unexpectedly, discrete six-coordinate platinum–thallium complex $Tl_2Pt(CN)_4$,[41] there has been a growing interest in the chemical and photophysical properties of heteropolynuclear Tl^I complexes.[5,42–50] Of particular note are a peculiar paramagnetic $[Tl\{PtR_4\}_2]^{2-}$ derivative containing a formal Tl^{II} center[51] and the series of complexes reported by Glaser and co-workers generated from the reaction between Pt^{II} substrates and Tl^{III} salts in which the sum of the oxidation states of the two metals is five.[52–54] Many of these complexes, particularly those containing Tl^I, have been shown to display luminescent properties, which have invariably been attributed to intermetallic interactions; however, a number of $Pt^{II,0}$–Tl^I complexes with strong Pt–Tl interactions do not exhibit any detectable emission.[55,56]

Abstract in Spanish: *Se ha sintetizado una nueva serie de complejos $[PtTl_2(C\equiv CR)_4]_n$ (n=2, R=4-$CH_3C_6H_4$ (Tol) **1**, 1-naftil (Np) **2**; n=∞, R=4-$CF_3C_6H_4$ (Tol_F) **3**) por neutralización entre Tl^I ($TlNO_3$ o $TlPF_6$) y los sustratos de platino $[Pt(C\equiv CR)_4]^{2-}$ (R=Tol, Tol_F) ya descritos o el nuevo $(NBu_4)_2[Pt(C\equiv CNp)_4]$. Asimismo, se han resuelto, mediante estudios de difracción de rayos-X, las estructuras cristalinas de $[Pt_2Tl_4(C\equiv CTol)_8]\cdot 4$ acetona, **1**·4 acetona, $[Pt_2Tl_4(C\equiv CNp)_8]\cdot 3$ acetona·$^1/_3H_2O$, **2**·3 acetona·$^1/_3H_2O$, y $[\{PtTl_2(C\equiv CTol_F)_4\}(acetona)S]_\infty$ (S=acetona **3a**; dioxano **3b**). Curiosamente, mientras que en los derivados de tolilo (**1**) y naftilo (**2**), los centros metálicos de talio exhiben una clara preferencia de enlace hacia los fragmentos básicos acetilénicos, dando lugar a redes cristalinas basadas en oligómeros hexanucleares de tipo sándwich $[Pt_2Tl_4(C\equiv CR)_8]$ (con interacciones secundarias adicionales Tl···acetona, **1**, o Tl···naftilo, **2**), en los derivados con $C_6H_4CF_3$ (TolF), **3a** y **3b**, el centro básico de Pt^{II} forma dos enlaces Pt-Tl no soportados. Como consecuencia, **3a** y **3b** forman una estructura columnar extendida, basada en la conexión, a través de interacciones secundarias Tl···η^2(acetileno), de unidades trimetálicas "$PtTl_2(C\equiv CTol_F)_4$" desplazadas entre sí. Además, se han estudiado las propiedades luminiscentes, que difieren mucho en disolución (azul; CH_2Cl_2 **1**,**2**; acetona **3**) a estado sólido (naranja). De manera interesante, la emisión de **1** en estado sólido depende de la presencia de acetona (verde), así como de su cristalinidad. Por otro lado, mientras que una muestra pulverulenta de **3** es de color amarillo pálido y muestra emisiones en el azul (457 nm) y naranja (611 nm), las pastillas obtenidas por presión (KBr o sólido puro), o, incluso, el polvo fino obtenido por molturación, son de color naranja y exhiben solamente una emisión intensa en el naranja (590 nm).*

In the past two decades, much has been discovered about the photoluminescence behavior of alkynylplatinum(II) complexes,[57–62] but, in comparison, relatively little is understood about the emissive properties of heteropolynuclear platinum systems containing alkynyl bridging ligands.[63–66] Recent studies by us[67–70] and others[63,66] have shown that their luminescence behavior can be modulated through metal···metal and η^2-alkynyl–metal bonding interactions. Within this framework, we have recently reported that the homoleptic derivatives $[Pt(C\equiv CR)_4]^{2-}$ (R = *t*Bu, Ph, $SiMe_3$) produce unexpected hexanuclear luminescent complexes of the type $[Pt_2Tl_4(C\equiv CR)_8]$ by sandwiching naked Tl^I centers through Tl^I–alkyne interactions,[71] thus indicating that in these systems the Tl^I centers have a stronger preference for the electron-rich alkynyl entities than for the basic Pt^{II} center. Surprisingly, in similar reactions with heteroleptic *cis*- or *trans*-platinate systems $[Pt(C_6F_5)_2(C\equiv CR)_2]^{2-}$ (R = *t*Bu, Ph), the platinum center has a higher affinity for thallium than for the alkynyl ligands, yielding six-coordinate platinum entities with two direct Pt–Tl bonds that dimerize ([{*trans*,*cis*,*cis*-$PtTl_2(C_6F_5)_2(C\equiv CPh)_2\}_2$])[72] or polymerize ([{*trans*,*trans*,*trans*-$PtTl_2(C_6F_5)_2(C\equiv Ct\text{Bu})_2\}_n$]),[73] in these cases through secondary Tl^I–alkynyl(C-α) contacts. These results suggest that the presence of two electron-withdrawing C_6F_5 groups in the mixed systems probably stabilizes the platinum fragment, favoring the interaction between the platinum and thallium orbitals (Pt $5d_{z^2}$, Tl $6s^2$ filled; Pt, Tl $6p_z$ empty). With all this knowledge, we thought it would be of interest to compare the ability of $[Pt(C\equiv C\text{-aryl})_4]^{2-}$ (aryl = Tol, Tol_F), which contain electron-donating (CH_3) and electron-withdrawing (CF_3) substituents on the arylethynyl group, and $(NBu_4)_2[Pt(C\equiv C\text{-Np})_4]$ to bind the Tl^I center.

Herein we report on the properties and structures of two novel hexanuclear Pt^{II}–Tl^I-alkynyl-based clusters $[PtTl_2(C\equiv CR)_4]$ (R = Tol **1**, Np **2**) and those of two unexpected supramolecular columnar species $[PtTl_2(C\equiv CTol_F)_4(acetone)S]_\infty$ (S = acetone **3a**, dioxane **3b**), the latter being formed by octahedral trimetallic entities connected through Tl···η^2-alkynyl bonding interactions.

Results and Discussion

Spectroscopic characterization: As shown in Scheme 1, complexes **1**–**3** were prepared as orange-yellow (**1**, **2**) or pale yellow (**3**) solids by treatment of aqueous solutions of the corresponding anionic platinate species $Li_2[Pt(C\equiv CR)_4]$ with $TlNO_3$ (1:2 molar ratio). The naphthyl derivative is only slightly soluble in CH_2Cl_2 and $CHCl_3$, and crystals suitable for X-ray diffraction (**2**·3 acetone·$^1/_3H_2O$) were obtained by slow diffusion of an acetone solution of $TlPF_6$ into a solution of $(NBu_4)_2[Pt(C\equiv CNp)_4]$ in acetone. Crystals of **1**·4 acetone were prepared by slow diffusion of acetone into a solution of compound **1** in tetrahydrofuran. Complex **3** is only soluble in acetone and from this solution pale yellow crystals of stoichiometry $[PtTl_2(C\equiv CTol_F)_4(acetone)_2]_\infty$ (**3a**) were obtained by slow evaporation of the acetone solution at 0 °C.

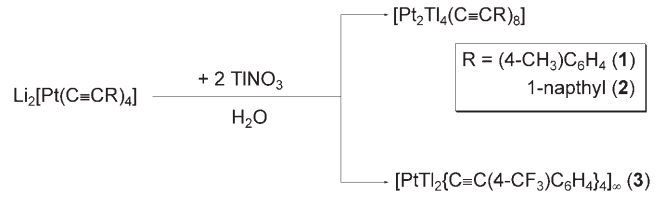

Scheme 1.

Evaporation of a solution of **3** in a mixture of acetone/dioxane (5:1) at room temperature yielded crystals of $[PtTl_2(C{\equiv}CTol_F)_4(acetone)(dioxane)]_\infty$ (**3b**). The ions $[Pt_2Tl_4(C{\equiv}CTol)_8+Tl]^+$ ($[M+Tl]^+$) and $[PtTl(C{\equiv}CTol_F)_4]^+$ ($[M-Tl]^+$) dominate the respective FAB(+) and ES(+) mass spectra of **1** and **3**, respectively. The IR spectra display very strong ν(C≡C) stretching vibrations (2086 cm^{-1}, R = Tol (**1**); 2079 cm^{-1}, R = Np (**2**); 2089 cm^{-1}, R = Tol_F (**3**)) that are slightly shifted to a higher wavenumber with respect to those observed for the homoleptic platinates $[NBu_4]_2[Pt(C{\equiv}CR)_4]$ (2082 cm^{-1}, R = Tol; 2065 cm^{-1}, R = Np; 2084 cm^{-1}, R = Tol_F). This spectroscopic feature has been previously observed in the hexanuclear clusters of $[Pt_2Tl_4(C{\equiv}CR)_8]$ (R = Ph, *t*Bu, $SiMe_3$),[71] and can tentatively be related to the small η^2-covalent contribution to the Tl^I–acetylenic bonding interactions, the electrostatic interaction between the platinate entities and the Tl^I centers probably being the driving force and the main contribution to the stability of these species. Interaction of naked metal (Ni^0[74,75] and Pt^0[76]), cations (Cu^I, Ag^I)[77] or M′Ln fragments[77,78] with metal-acetylenic entities LnMC≡CR usually causes a shift of the ν(C≡C) absorption to lower wavenumbers. The size of the $\Delta\tilde{\nu}$ shift relative to the precursor is related to the extent of the interaction with the M–C(α)≡C(β)–R entity. Larger shifts are observed with symmetrical and asymmetrical (with M′ being closer to the β-carbon atom) side-on η^2-bonding interactions, while small or negligible shifts are found when the interactions occur with the α-carbon atom (or M–C(α) fragment), leading to the final μ_n:η^1-C≡CR bridging ligands. In these platinum–thallium(I) complexes, the small shifts to higher frequencies suggest that the interaction between the platinate entities and the thallium centers decreases somewhat the π-back-donor component (Pt→π*C≡CR) in the $[Pt(C{\equiv}CR)_4]^{2-}$ fragments. In the $^{13}C\{^1H\}$ NMR spectrum of hexanuclear complex **1**, both the C-α and C-β alkyne resonances are downfield-shifted ($\delta C_\alpha = 117.5$ ppm, $\delta C_\beta = 109.6$ ppm) with regard to those found in $[NBu_4]_2[Pt(C{\equiv}CTol)_4]$ ($\delta C_\alpha = 114.5$ ppm, $\delta C_\beta = 103.2$ ppm), but despite prolonged accumulation, platinum satellites were not found. In contrast, the $^{13}C\{^1H\}$ NMR spectrum of complex **3** in [D_6]acetone shows the expected acetylenic resonances with ^{195}Pt satellites at 115.8 (C_α, $^1J(Pt,C\text{-}\alpha) = 981$ Hz) and 115.6 ppm (C-β, $^2J(Pt,C\text{-}\beta) = 273$ Hz), respectively. In this case, the two resonances are notably shifted upfield (C-α) and downfield (C-β), respectively, with respect to those of the precursor $[NBu_4]_2[Pt(C{\equiv}CTol_F)_4]$ ($\delta_{C\text{-}\alpha} = 125$ ppm, $^1J(Pt,C\text{-}\alpha) = 997$ Hz; $\delta_{C\text{-}\beta} = 103$ ppm, $^2J(Pt,C_\beta) = 286$ Hz). However, the platinum coupling constants are only slightly smaller than those of the precursor.

Crystal structures: The X-ray crystal structures of **1**·4 acetone, **2**·3 acetone·$^1/_3$ H_2O, **3a** and **3b** have been determined. Based on these structures, they can be classified into two types: hexanuclear clusters (**1** and **2**) and infinite $PtTl_2$ chains (**3a** and **3b**). Selected bond lengths and angles are presented in Table 1 and Table 2. The perspective views of the hexanuclear clusters **1** and **2** are depicted in Figure 1 and Figure 2, respectively. Complex **1**·4 acetone crystallizes in the $P\bar{1}$ space group, with one half of **1** and two molecules of acetone in the asymmetric unit, while complex **2**·3 acetone·$^1/_3$ H_2O crystallizes in the cubic $Ia\bar{3}d$ space group. Both complexes are formed from two eclipsed tetraalkynylplatinate fragments connected to four thallium centers in a sandwich fashion. Although the sandwich-type coordination of a single Tl^I center by clusters or polynuclear units has several precedents,[48,79] and even $[Tl\{Pt(C_6F_5)_4\}_2]^{2-}$ has been described, a very peculiar trinuclear derivative containing a $[Pt_2Tl]^{6+}$ skeleton,[51] the intercalation of several Tl^I centers by metal entities is very rare.[46,71] In both cases, each thallium center bisects the alkynyl entities, being bonded to four

Table 1. Selected bond lengths [Å] and angles [°] for $[Pt_2Tl_4(C{\equiv}CTol)_8]$·4 acetone (**1**·4 acetone) and $[Pt_2Tl_4(C{\equiv}CNp)_8]$·3 acetone·$^1/_3$ H_2O (**2**·3 acetone·$^1/_3$ H_2O).

	1·4 acetone	**2**·3 acetone·$^1/_3$ H_2O
Pt–C(α)	2.000(8)–2.014(8)	2.01(2), 2.03(3)
C(α)–C(β)	1.205(11)–1.221(10)	1.20(3)–1.24(3)
Pt–Tl	3.5675(5)–3.7204(4)	3.628(1)–3.714(1)
Pt···Pt	3.8463(5)	3.572(2)
Tl···Tl	4.3065(5), 4.4731(4)	4.538(1)
Tl–C(α)	2.900(7)–3.015(7)	2.91(2), 2.97(2)
Tl–C(β)	3.086(7)–3.296(10)	3.21(2)–3.29(2)
cis-C(α)–Pt–C′(α)	88.3(3)–91.7(3)	89.0(9)–90.6(9)
Pt–C(α)–C(β)	173.0(7)–178.2(6)	172(2), 172.3(18)
C(α)–C(β)–C_{ipso}	175.8(8)–179.5(8)	177(3), 179(3)

Table 2. Selected bond lengths [Å] and angles [°] for $[\{PtTl_2(C{\equiv}CTol_F)_4\}$(acetone)(dioxane)$]_\infty$ (**3b**).

	3b
Pt–C(α)	2.009(9)–2.020(9)
C(α)–C(β)	1.192(11)–1.206(11)
Pt–Tl1	2.9355(5)
Pt–Tl2	3.0272(5)
Tl1–O1	2.823(11)
Tl2–O3	2.924(11)
Tl–C(α)	3.034(10)–3.121(8)
Tl–C(β)	2.980(10)–3.131(10)
cis-C(α)–Pt–C′(α)	87.8(4)–92.2(3)
Pt–C(α)–C(β)	175.2(8)–179.9(9)
C(α)–C(β)–C_{ipso}	174.8(9)–179.4(11)

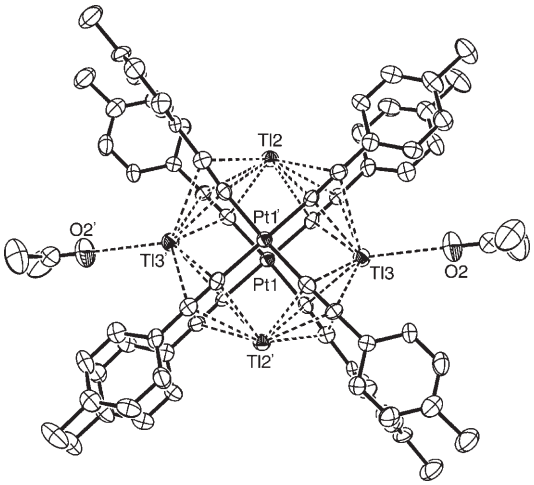

Figure 1. Molecular structure of the hexanuclear cluster $[Pt_2Tl_4(C{\equiv}CTol)_8]$ (**1**) showing the contacts of two thallium atoms with two acetone molecules. Ellipsoids are drawn at the 50% probability level. Hydrogen atoms are omitted for clarity.

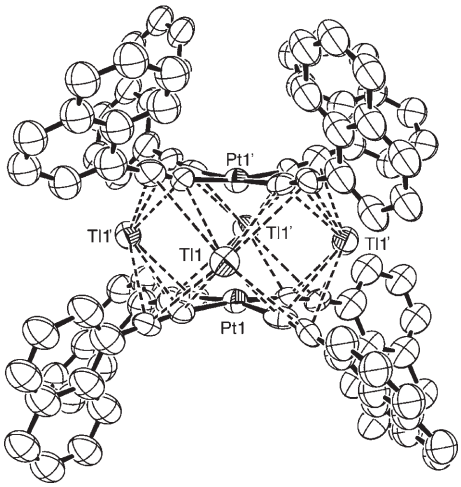

Figure 2. ORTEP view of the hexanuclear cluster $[Pt_2Tl_4(C{\equiv}CNp)_8]$ (**2**). Ellipsoids are drawn at the 50% probability level. Hydrogen atoms are omitted for clarity.

alkynyl fragments (two associated with each platinum unit), which display a μ_3-η^2(σ-Pt, π-Tl, π-Tl) bonding mode. As can be observed in Figure 2, the alkynyl fragments in the naphthyl derivative are tilted away from the thallium centers (Pt–C(α)–C_β 172(2), 172.3(18)°; C(α)–C(β)–C(γ) 177(3), 179(3)°), with the aromatic naphthyl groups forming dihedral angles of 47.2(6) and 75.1(6)° with their respective platinum coordination plane and producing two clear cavities (one associated with each platinum atom). In the extended crystal lattice, molecules of **2** are arranged as shown in Figure 3. No apparent intermolecular π···π contacts are observed between the naphthyl groups. A perspective view of the lattice (see the Supporting Information, Figure S1) indicates that the shortest intermolecular contact is made by the thallium centers, each one being engaged in a very weak

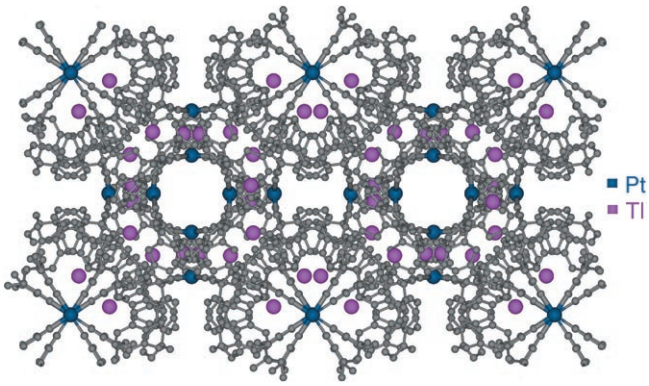

Figure 3. Expansion of the crystalline structure of $[Pt_2Tl_4(C{\equiv}CNp)_8]{\cdot}3$ acetone$\cdot^1/_3 H_2O$ (**2**·3 acetone·$^1/_3 H_2O$).

π···Tl interaction with a naphthyl group of a neighboring cluster. In particular, the distances of the thallium atom to three consecutive carbon atoms (Tl1–C17 3.711, Tl1–C18 3.411, Tl1–C19 3.842 Å) fit well with the reported range for arene···thallium contacts (2.87–3.74 Å).[80–84] The acetone molecules are trapped in the circular void channels of the crystal lattice (Figure 3), but they do not show any significant interactions with the hexanuclear $PtTl_4$ clusters.

In the hexanuclear tolyl derivative **1**·4 acetone, three of the tolyl groups remain practically coplanar with the platinum coordination plane and the resulting clusters stack in columns along the *a* axis (intermolecular Pt···Pt separation 7.368 Å), yielding channels in which the acetone molecules are located. In this cluster one of the two solvent acetone molecules found in the asymmetric unit is weakly coordinated to a thallium center with a Tl–O separation of 3.042(9) Å, clearly longer than similar Tl–O(acetone) distances observed in other heteropolynuclear thallium complexes[45,72,73] (see Figure 1). Note that the incorporation of acetone in solid **1** causes a visual color change from orange to yellow, but the acetone molecules are rapidly lost when the solid is air-dried. Nevertheless, it is noteworthy that the resulting dull yellow-orange solid is very insoluble in all common organic solvents. In this insoluble phase the Tl··· acetone contacts are probably substituted by efficient Tl···arene(Tol) interactions similar to those observed in the naphthyl derivative, which is also very insoluble in organic solvents. In its IR spectrum the ν(C≡C) band is only slightly shifted ($\Delta\tilde{\nu}(\nu(C{\equiv}C)) = 4\ cm^{-1}$) to higher wavenumbers, and no absorption due to the presence of acetone is observed.

The η^2-acetylenic–Tl interactions are asymmetric in both complexes **1** and **2**, the Tl–C(α) distances (range 2.900–3.015 Å for **1**, 2.91–2.97 Å for **2**) being notably shorter than the corresponding Tl–C(β) contacts (3.086–3.296 Å for **1**, 3.21–3.29 Å for **2**). These distances are very close to the sum of the van der Waals radius of carbon (1.7 Å) and the ionic radius of Tl^+ (1.4–1.5 Å), suggesting a notable ionic contribution to the bonding interaction in this type of assembly. As expected, the shortest Tl–C(α) contacts (2.900–2.936 Å) in complex **1** are formed by Tl2, probably as a result of the additional weak contact of Tl3 with the acetone molecule.

The intramolecular Pt···Pt separation found between the two platinum fragments is notably shorter in the naphthyl derivative (Pt···Pt = 3.572(2) Å in **2** vs. 3.8463(5) Å in **1**). The value of 3.572(2) Å is similar to that previously reported for $[Pt_2Tl_4(C{\equiv}Ct\mathrm{Bu})_8]$ (3.573 Å molecule A; 3.622 Å molecule B),[71] and comparable to those seen in linear-chain Pt^{II} complexes (3.01–3.75 Å).[25–32,69,71] In both complexes **1** and **2**, the Pt···Tl distances (3.5675–3.7204 Å in **1**; 3.628(1) and 3.714(1) Å in **2**) lie out of the usual range of Pt^{II}–Tl^{I} bond lengths,[41,50,72,73] which suggests that only weak metal···metal bonding interactions occur (sum of the van der Waals radii = 3.68 Å). The very long Tl···Tl separations (see Table 1) rule out any intramolecular Tl···Tl bonding interactions.

Crystals of the adduct $[PtTl_2(C{\equiv}CTol_F)_4(acetone)_2]_\infty$ (**3a**) systematically diffracted poorly and lost solvent of crystallization very easily, even when covered with mineral oil at a low temperature. Nevertheless, in spite of the lack of accuracy of the crystallographic analyses performed on **3a**, the formation of a supramolecular structure based on $PtTl_2$ units, nearly identical to that observed for the adduct $[PtTl_2(C{\equiv}CTol_F)_4(acetone)(dioxane)]_\infty$ (**3b**) (one acetone occupies the site of the dioxane molecule), was unequivocally confirmed. In the *p*-trifluoromethylphenyl derivative **3b**, the acceptor CF_3 substituent reduces the electron density at the acetylenic units, making the basic platinum center the preferred binding site. In addition, as commented in the introduction, the presence of four electron-withdrawing acetylide C≡C(4-$CF_3C_6H_4$) ligands could also increase the metallophilic attraction between Pt^{II} and Tl^{I}. Thus, the molecular structure reveals a pseudo-octahedral platinum center (Figure 4a) with two donor–acceptor Pt–Tl bonds (Pt–Tl 2.9355(5), 3.0272(5) Å). Individual trimetallic $[PtTl_2(C{\equiv}CR)_4]$ fragments self-associate through Tl···π-alkynyl interactions to yield an unusual columnar superstructure along the *a* axis. The association is based on interactions between each thallium atom and two mutually *cis*-alkynyl fragments of a neighboring trimetallic $PtTl_2$ entity (see the Supporting Information, Figure S2). As can be seen, the extended structure can alternatively be described as a continuous stack of $[Pt(C{\equiv}CTol_F)_4]^{2-}$ ions with the platinum centers offset to form a zigzag chain (Pt···Pt···Pt 128.74°, Figure 4b) in order to accommodate the two Pt–Tl bonds and to maximize the alkynyl···thallium bonding interactions. In the final structure two noncontacting thallium centers [Tl1···Tl1′ 4.3906(7), Tl2···Tl2′ 5.2161(6) Å) are sandwiched between the platinate anions. The columnar structure exhibits alternating long (5.16 Å) and short (4.29 Å) separations between the platinate anions owing to the presence of two different thallium centers (Tl1 and Tl2). As shown in Figure 4a, while the Tl(1) atom located above the platinum center (Pt–Tl1 2.9355(5) Å) is essentially perpendicular to the platinum coordination plane (angle with the normal = 2.0(2)° in **3b**), the other thallium center Tl2, located below it, exhibits a Pt–Tl2 distance that is slightly longer (3.0272(5) Å) and the Pt–Tl2 vector is perceptibly displaced from the normal by 21.9(2)°. The resulting Tl1-Pt-Tl2 angle is 160.044(17)°. As a consequence, while the Tl1 atom only interacts with the two alkynyl fragments of the adjacent platinate stack (Tl1–C(α)/C(β) 3.073(11), 3.099(9)/2.980(10), 3.020(9) Å; see the Supporting Information, Figure S2a), the Tl2 atom seems to interact additionally with two alkynyl groups of its own entity, as suggested by the relatively short distances observed between the Tl(2) and the C(α) atoms (Tl2–C1/C10 3.072(8)/3.267(9) Å; see the Supporting Information, Figure S2b). The displacement of Tl2 towards the alkynyl groups favors the proximity of the platinate anions (a distance of 4.29 Å vs a value of 5.16 Å, corresponding to platinate fragments separated by Tl1 centers). As is shown in Figure S2 in the Supporting Information, both thallium centers complete their coordination environment by forming weak contacts with solvent molecules (Tl1···O1(dioxane) 2.823(11), Tl2···O3(acetone) 2.924(11) Å). Note that the solvent molecules are located in channels that are parallel to the resulting $[PtTl_2(C{\equiv}CTol_F)_4]$ columns (see the Supporting Information, Figure S3) and are easily lost when the crystals are dried.

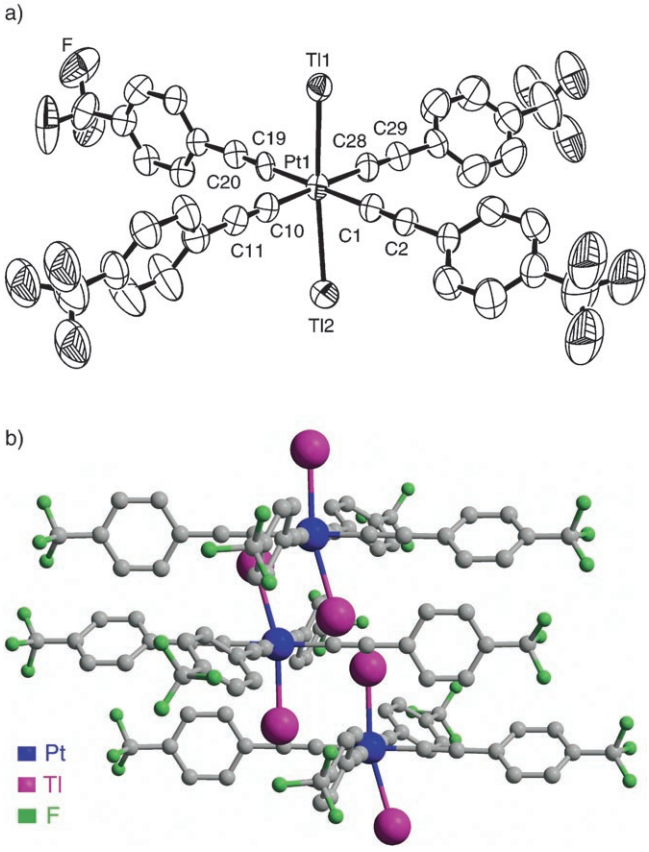

Figure 4. a) ORTEP view of the pseudo-octahedral environment of the platinum atom in complex $[PtTl_2(C{\equiv}CTol_F)_4(acetone)(dioxane)]_\infty$ (**3b**). Ellipsoids are drawn at the 50% probability level. Hydrogen atoms, as well as the coordination molecules of acetone and dioxane, are omitted for clarity. b) Perspective view along the *a* axis of the crystalline structure showing the stacking of the $[PtTl_2(C{\equiv}CTol_F)_4]$ units.

Absorption and emission spectroscopy: As was mentioned above, complex **2** (R = Np) is only slightly soluble in chlori-

nated solvents (CH_2Cl_2, $CHCl_3$), and complex **3** ($R = Tol_F$) only in acetone. Freshly prepared complex **1** is soluble in a range of solvents (chloroform, THF and CH_2Cl_2), but is scarcely soluble in acetone and, once it has been treated with acetone, the resulting dried solid is insoluble in all common organic solvents. Note also that the conductivities of $[Pt_2Tl_4(C{\equiv}CTol)_8]$ (**1**) (acetone solution, 1.5 $cm^2\,\Omega^{-1}\,mol^{-1}$; CH_2Cl_2 solution, 1 $cm^2\,\Omega^{-1}\,mol^{-1}$), and that of $[Pt_2Tl_4(C{\equiv}CTol_F)_8]$ (**3**) (acetone solution, 15 $cm^2\,\Omega^{-1}\,mol^{-1}$) indicate that the thallium ion does not dissociate in solution to any appreciable extent. This suggests that the $PtTl_2$ units of complex **3** are largely retained when dissolved and that the hexanuclear cluster Pt_2Tl_4 of complex **1** is also present in solution. The electronic absorption data for **1**–**3** are summarized in Table 3 and the electronic spectra of these complexes together with those of the corresponding precursors are shown in the Supporting Information (Figure S4). The electronic spectrum of **1** is similar to that of $(NBu_4)_2[Pt(C{\equiv}CTol)_4]$ for $\lambda < 360$ nm, but differs dramatically by exhibiting a novel prominent low-energy absorption at 380 nm. The high-energy bands (270–326 nm) and the absorption at 360 nm are ascribed to intraligand (IL) $\pi\rightarrow\pi^*$ and mixed $\pi\rightarrow\pi^*(C{\equiv}CR)$IL/d(Pt)$\rightarrow\pi^*(C{\equiv}CR)$ MLCT transitions, respectively. The novel, prominent low-energy absorption at 380 nm, which is absent in the precursor and is slightly solvent-dependent, is tentatively assigned to a metal–alkynyl-to-metal cluster core $[Pt(C{\equiv}CR)_4\rightarrow Pt_2Tl_4]$ MLM′CT transition in accord with previous assignments in related systems.[63,71] In acetone, the $PtTl_2$ complex **3** shows two absorption bands at 328 and 360 nm, which are similar in energy to those observed for the homoleptic derivative $(NBu_4)_2[Pt(C{\equiv}CTol_F)_4]$ (329, 354 nm), and a novel moderately intense lower-energy band at 376 nm, related to the presence of Pt–Tl bonds. At concentrations higher than 5×10^{-4} mol L^{-1}, a weak shoulder at $\lambda_{max} = 445$ nm ($\varepsilon \approx 0.7\times10^3$ L $mol^{-1}\,cm^{-1}$), which obeys Beer's law (in the 5×10^{-4} to 2.7×10^{-3} mol L^{-1} range[85]) and can be regarded as the spin-forbidden counterpart of the intense band, is clearly observed (see the Supporting Information, Figure S5). The inferred singlet–triplet excited-state splitting (4124 cm^{-1}) is comparable to the values observed in other polynuclear complexes that contain metal···Tl bonds, in which the low-energy absorption is assigned to a metal-centred transition $\sigma^*[M(d)Tl(s)]\rightarrow\sigma[M,Tl(p_z)]$.[42,86] Previous theoretical studies on model $[PtTl_2Ph_2(C{\equiv}CPh)_2]$ and $[PtTlPh_2(C{\equiv}CPh)_2]^-$ complexes[72] with Pt–Tl bonds indicate that the $[PtPh_2(C{\equiv}CPh)_2]$ fragments play a significant role in the highest-occupied orbitals, while the $PtTl_2$ or PtTl units make a notable contribution to the lowest-unoccupied orbitals. Similarly, we suggest that in complex **3** this band can be tentatively attributed to metal–alkynyl-to-metal charge transfer $[Pt/C{\equiv}CR\rightarrow\sigma[Pt,Tl(p_z)]$, although some mixing of the target orbital with $\pi^*C{\equiv}CR$ cannot be excluded.

Table 3. Absorption data for complexes **1**–**3** and $(NBu_4)_2[Pt(C{\equiv}CNp)_4]$ (**A**) ($\approx 5\times10^{-5}$ M).

Compound	Absorption [nm] (ε [10^3 L $mol^{-1}\,cm^{-1}$])
1[a]	327 (17.5), 360 (14.3), 380 (23.3) (acetone)
	270 (44.9), 295 (37.4)(sh), 326 (16.5), 360 (10.9), 383 (19.6) (CH_2Cl_2)
2	242 (66.0), 320 (46.2), 338 (50.8), 399 (25.8) (CH_2Cl_2)
3	328 (15.8), 360 (14.9), 376 (15.1), 445 (0.7)[b] (acetone)
A	240 (55.0), 260 (38.9), 340 (26.32)(sh), 360 (35.7)(sh),
	378 (43.3)(sh), 396 (51.5)

[a] With a long tail extending to about 450 nm. [b] For $[\mathbf{3}] = 5\times10^{-4}$ mol L^{-1} or higher.

The emission data for complexes **1**–**3** are summarized in Table 4. For the tolylacetylide derivative **1**, the luminescence differs in the solid state and in solution. To illustrate this, the solid (298 K) and solution (CH_2Cl_2) emission and excitation spectra of **1** are presented in Figure 5. In solution, complex **1** emits at $\lambda = 478$ nm (asymmetric band) and its excitation spectrum is comparable to its absorption spectrum. Upon cooling to 77 K, λ_{em}^{max} shifts to a slightly shorter wavelength (472 nm) and is clearly structured with vibronic progression (1960–1990 cm^{-1}) typical of the $\nu(C{\equiv}C)$ stretching modes and indicative of the involvement of alkynyl ligands in the excited state. This emission is similar to that observed for the homoleptic precursor $[(NBu_4)_2[Pt(C{\equiv}CTol)_4]$ [λ_{em}^{max} (77 K) = 447 nm],[57] but with a lower energy ($\Delta = 1185$ cm^{-1}). Similar behavior was observed in acetone (see Table 4). Conductivity measurements and the FAB(+) mass spectrum of **1**, which shows a peak at 2333 a.m.u. corresponding to the ion $[M+Tl]^+$, suggest that the integrity of the clusters is probably retained in solution. Therefore, although a definitive assignment is not possible, the emissive state in solution is likely to be derived from a mixed IL ($\pi\rightarrow\pi^*C{\equiv}CR$) and a metal–ligand-to-metal cluster core transition ^{3}MLM′CT $[Pt(C{\equiv}CR)_4\rightarrow Pt_2Tl_4]$. In the solid state, the cluster of complex **1** displays strong orange luminescence whose maximum slightly red shifts from about 590 to 602 nm by increasing λ_{exc} from 370 to 490 nm. Similar site-selectivity excitation was also observed at 77 K, with the peak maxima ranging from 587 to 621 nm (for $\lambda_{exc} = 370$–490 nm). Luminescence lifetime measurements fit reasonably well to one component with a lifetime of approximately 12.0 μs [298 K; 12.3(±0.2) μs ($R^2 = 0.99142$) at $\lambda_{max} = 590$ nm, and 11.5(±0.3) μs ($R^2 = 0.98647$) at $\lambda_{max} = 602$ nm],[87] which is consistent with a predominantly spin-forbidden process. The onset of the excitation spectrum, which is also slightly different when monitored at 590 nm ($\lambda_{max} = 490$ nm, Figure 5) compared with that monitored at 650 nm ($\lambda_{max} = 494$ nm), appears well before the onset of the absorption spectrum, suggesting that the luminescence properties in the solid state are probably related to the existence of aggregates of clusters. Different degrees of aggregation could explain the slight shifts observed in both the emission and excitation spectra. In agreement with this suggestion we have noticed that, to the naked eye, a crystalline sample of

Table 4. Emission and excitation data for complexes **1**–**3** and $(NBu_4)_2[Pt(C{\equiv}CNp)_4]$ (**A**).

		λ_{exc}^{max} [nm]	λ_{em}^{max} [nm]	τ [μs]
1	solid (298 K)[a]	370, 442, 434, 490 ($\lambda_{em}=590$ nm)	590 ($\lambda_{exc}=370$ nm)	12.0
		367, 494 ($\lambda_{em}=650$ nm)	602 ($\lambda_{exc}=490$ nm)	
	solid (77 K)[a]	370(min), 472, 487(sh) ($\lambda_{em}=620$ nm)	587 ($\lambda_{exc}=370$ nm)	16.4
			605 ($\lambda_{exc}=470$ nm)	
			621 ($\lambda_{exc}=490$ nm)	
	CH_2Cl_2, 5×10^{-4} M (298 K)[b,c]	342, 365, 403 ($\lambda_{em}=480$ nm)	478	
	CH_2Cl_2, 5×10^{-4} M (77 K)	310–390, 447(sh)	472, 520, 580	20.9, 172.0
2	solid (298 K)	no emission	no emission	
	solid (77 K)	370, 501, 543	580, 627(sh)	115.0
	CH_2Cl_2, 10^{-3} M (77 K)[d]	350, 406, 428	554, 602, 621, 655	172.4
3	KBr (298 K)	354(min), 400, 449, 458, 465(sh)	587	10.4
	KBr (77 K)	353(min), 379, 445, 455, 472(sh)	591	16.8
	solid (298 K)	331(min), 420, 433, 445(sh) ($\lambda_{em}=460$, 590 nm)	457*, 497(sh), 611· ($\lambda_{exc}=390$ nm)	*10.0, ·9.8
	solid (77 K)	379, 428, 463(sh) ($\lambda_{em}=617$ nm)	462*, 615· ($\lambda_{exc}=390$ nm)	*12.8, ·15.7
		355, 376, 390, 425(sh)(λ_{em}=465 nm)		
	acetone, 5×10^{-3} M (298 K)[e]	435, 454(sh) ($\lambda_{em}=585$ nm)	470, 512(sh), 584(max) ($\lambda_{exc}=425$ nm)	
	acetone, 5×10^{-3} M (77 K)	366, 440, 462(max) ($\lambda_{em}=590$ nm)	613 ($\lambda_{exc}=466$ nm)	
		320, 356, 374(max), 430, 445, 455 ($\lambda_{em}=466$ nm)	466*, 515, 580·(min) ($\lambda_{exc}=375$ nm)	*28.9, ·232.1
A	CH_2Cl_2, 10^{-3} M (77 K)[f,g]	370–549	565, 579(sh), 613, 638	165.8

[a] The same results were obtained in KBr pellets. [b] The same results were obtained in acetone in very concentrated and for 5×10^{-4} M solutions [$\lambda_{max}=$ 475 nm (278 K); 470, 513, 570(sh) (77 K)]. [c] $\phi=8.1\times10^{-3}$. Measured using DCM [4-(dicyanomethylene)-2-methyl-6-(4-dimethylaminostyryl)-4*H*-pyran] as standard. [d] $\phi=8.2\times10^{-5}$. Measured using DCM as standard. [e] $\phi=7.2\times10^{-3}$. Measured using $[Ru(bipy)_3]Cl_2$ as standard. [f] As a solid, at 77 K, a weak emission with maxima at 565, 645 and 800 nm; the band at 800 nm is probably due to an excimeric emission ($\tau=58.2$ μs). [g] $\phi=8.7\times10^{-4}$. Measured using DCM as standard.

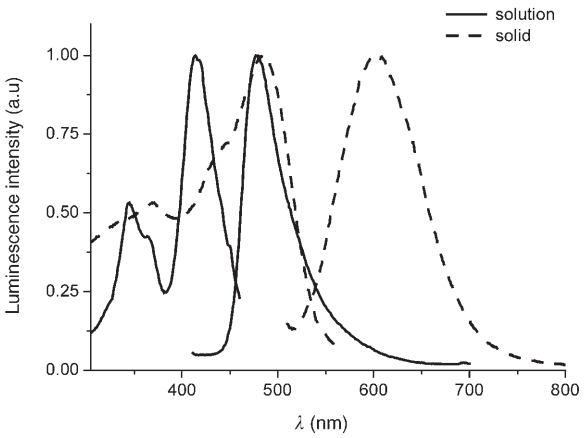

Figure 5. Excitation and emission spectra of **1** in the solid state and in CH_2Cl_2 solution ($[\mathbf{1}]=5\times10^{-4}$ mol L^{-1}) at room temperature.

1·4 acetone emits an intense green-yellow luminescence under UV illumination (298 K, $\lambda_{max}=479$, 521 nm ($\lambda_{exc}=$ 370 nm); 77 K, $\lambda_{max}=502$, 529, 563 nm ($\lambda_{exc}=460$ nm); see the Supporting Information, Figure S6), which is lost when the crystals are air-dried. The change in emission seems to arise from the interaction of Tl^I centers with acetone molecules, as shown in the crystal structure. A visual change from deep orange to yellow-green luminescence is also observed on exposure of a solid powder of **1** (yellow-orange) to acetone vapour. However, when the acetone is eliminated in a vacuum, a dull yellow-orange solid is generated, which does not show the initial orange luminescence. This fact precludes its use as a sensor. As previously commented, this latter solid has very low solubility in organic solvents and exhibits two emission bands at 485 and 590 nm ($\lambda_{exc}=$ 440 nm, see the Supporting Information, Figure S7).

Complex **2** only emits in rigid media at a low temperature. Thus, a weak orange emission [$\lambda_{max}=580$, 627(sh) nm] was observed in the solid state upon excitation between 370–540 nm at 77 K. In a frozen CH_2Cl_2 solution (77 K), the emission of **2** is shifted to a higher energy ($\lambda_{max}=554$ nm, $\tau=172.4$ μs) and is clearly structured. The striking similarity of the emission spectrum of **2** to that of its precursor $(NBu_4)_2[Pt(C{\equiv}CNp)_4]$, which also exhibits a vibronic emission ($\lambda_{max}=565$ nm, $\tau=165.8$ μs) in frozen CH_2Cl_2 solution, is suggestive of a similar emissive state. The vibrational progression spacings of about 1440 and 1950 cm^{-1} for **2** and 1385 and 2025 cm^{-1} for $(NBu_4)_2[Pt(C{\equiv}CNp)_4]$ are in agreement with a ligand-dominated emissive state, and the lowest emissive state in both derivatives is, therefore, assigned to a metal (or cluster)-perturbed intraligand π–π* transition. The absence of detectable emission for both complexes in the solid state at room temperature can be attributed to quenching by intermolecular π(naphthyl)···Tl^+ or π···π(naphthyl) interactions in the crystal lattice, which are seemingly retarded at low temperatures.

Compound **3** is an interesting example of a molecule whose color and emissive properties change with pressure. Thus, complex **3** is only soluble in acetone, and crystallises with acetone molecules (**3a**), which weakly interact with thallium centers, as a very pale yellow solid. The crystalline

solid loses the acetone molecules rapidly when isolated from solution (as observed by IR spectroscopy), but retains its pale yellow color. Similar behavior is observed for crystals of $[PtTl_2(C{\equiv}CTol_F)_4(acetone)(dioxane)]_\infty$ (**3b**). These solids display, regardless of the λ_{exc} used (350–400 nm), two luminescence bands at 457 and 611 nm. Upon cooling, the intensity of the emissions increases significantly and the emission shift slightly to lower energies (462 and 615 nm). As can be seen in Figure 6a, both bands have similar excitation profiles at $\lambda < 430$ nm but, by monitoring at 617 nm, an additional shoulder feature also appears at the position of the high-energy emission (463 nm). Lifetime measurements indicate that both bands are phosphorescent (see Table 4), but their wavelength dependence suggests that each emission derives from a different excited state. The close resemblance of the excitation profiles and the fact that the shoulder at 463 nm (77 K) of the low-energy excitation band (monitoring at 617 nm) coincides with the high-energy emission at 77 K (462 nm), indicates that the orange emission at approximately 615 nm has a contribution from the blue one at 462 nm. Interestingly, we have noted that by simply grinding the crystalline pale yellow samples of **3**, or by using 10 ton pressure to make KBr pellets, the initial pale yellow color changes to orange, and a very intense orange emission is produced under UV irradiation. Under these conditions, the blue emission is not observed and only a structureless low-energy band (KBr pellets: $\lambda_{max} = 587$ nm at 298 K, $\tau = 10.4$ μs; $\lambda_{max} = 591$ nm at 77 K, $\tau = 16.8$ μs, see Table 4; solid pellets: $\lambda_{max} = 608$ nm at 298 K, Figure S8 in the Supporting Information) appears, suggesting that the intersystem crossing (or mixing) from both emissive states is very efficient (see Figure 6b).

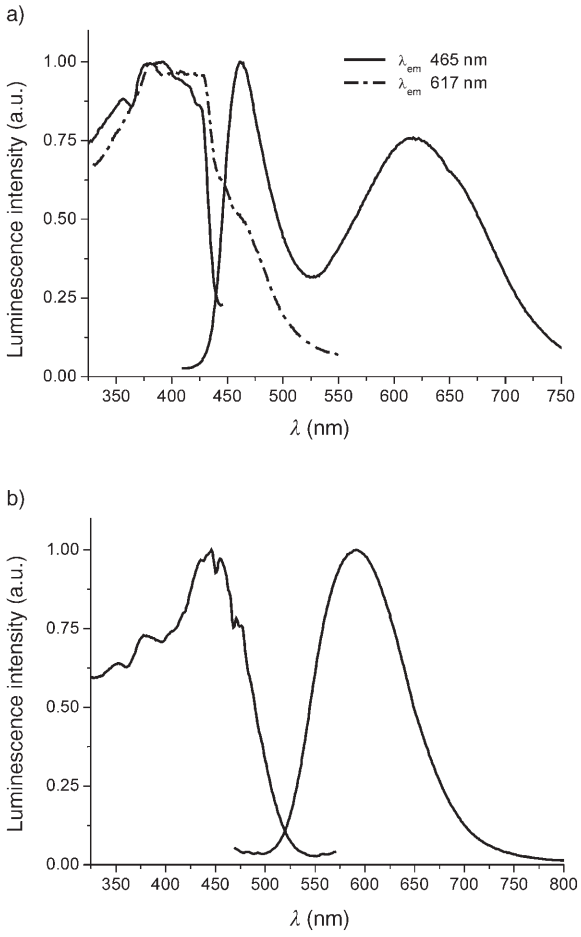

Figure 6. Excitation and emission spectra of **3** at 77 K in a) the solid state (powder) and b) KBr pellets.

The emissive behavior of **3** in acetone solution is sensitive to complex concentration. This fact is illustrated, at room temperature, in Figure 7. The complex exhibits a vibronic

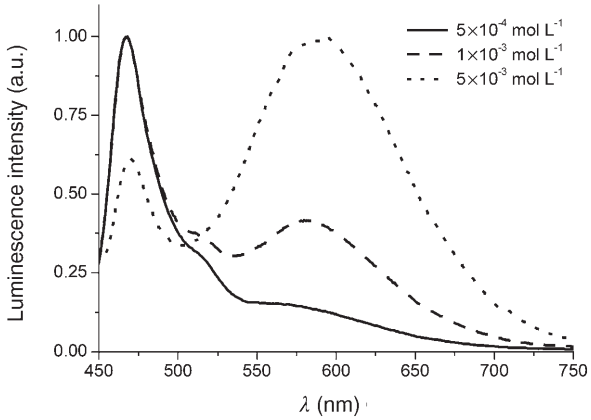

Figure 7. Variable concentration emission spectra of **3** in acetone at room temperature.

high-energy emission ($\lambda_{max} = 470$, 512 nm), which is better resolved in a frozen acetone solution ($\lambda_{max} = 466$, 515 nm, 77 K), and a broad low-energy feature ($\lambda_{max} = 584$ nm), which dominates the spectrum at concentrations of 5×10^{-3} mol L^{-1} or more and is nearly absent at a concentration of 5×10^{-4} mol L^{-1}. Similar behavior is observed in frozen solutions, with minor shifts of both emissions. To illustrate this, Figure 8 shows the emission spectra, with excitation at 375 and 466 nm, of a frozen solution of **3** at 77 K (5×10^{-3} M) and, also, the very different excitation profiles of both emissions. In this complex, the structured high-energy emission in fluid or glass acetone solution is comparable in energy to that recorded in the solid state for the pale yellow form, implying a common emissive state. The close resemblance of this high-energy emission to that seen in the homoleptic precursor $(NBu_4)_2[Pt(C{\equiv}CTol_F)_4]$ (acetone, $\lambda_{max} = 468$ nm) is suggestive of an emission with a predominantly intraligand $\pi \rightarrow \pi^*$ ($C{\equiv}CTol_F$, ^{3}IL) character. Notwithstanding, a certain degree of metal-to-ligand (^{3}MLCT) character cannot be ruled out. The strong orange emission seen in KBr, or solid sheen pellets (see the Supporting Information, Figure S8), and the low-energy band observed in powder solid and fluid or glass is thought to occur by lumophore aggregation of $[PtTl_2(C{\equiv}CR)_4]$ units through Tl···π(alkynyl) interactions.

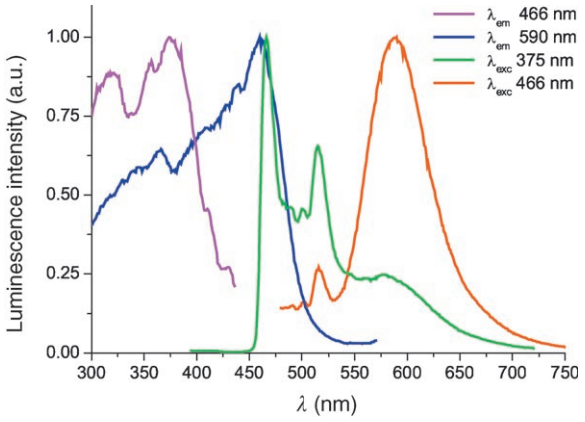

Figure 8. Excitation and emission spectra of **3** in acetone solution ([**3**] = 5×10^{-3} mol L^{-1}) at 77 K.

Experimental Section

Absorption and emission spectroscopy: The reactions were performed under argon and solvents were purified by standard methods. ^{1}H and ^{13}C NMR spectra were recorded with 300ARX and 400ARX Bruker spectrometers. Chemical shifts are reported in ppm relative to an external standard ($SiMe_4$) and all coupling constants are given in Hz. UV/Vis spectra were recorded with a Hitachi U-3400 spectrometer. Emission and excitation spectra were obtained with a Perkin-Elmer Luminescence Spectrometer LS 50B and on a Jobin-Yvon Horiba Fluorolog 3-22 Tau-3 spectrofluorimeter, with the lifetimes measured in phosphorimeter mode. The solution emission quantum yields were measured by the Demas and Crosby method[88] using $[Ru(bipy)_3]Cl_2$ in degassed water or DCM [4-dicyanomethylene-2-methyl-6-(4-dimethylaminostyryl)-4*H*-pyrane] in degassed methanol as standards. IR spectra were recorded with a Perkin-Elmer FT-IR Spectrum 1000 spectrometer and mass spectra with a HP-5989B spectrometer equipped with interphase API-ES HP-59987A (ES+) and a VG Autospec double-focussing (FAB+) mass spectrometer. Elemental analyses were performed with a Perkin-Elmer 2400 CHNS/O microanalyser. Conductivities were measured in acetone solutions (ca. 5×10^{-4} mol L^{-1}) using a Crison GLP31 conductimeter. The acetylenes were purchased and used without further purification. $[PtCl_2(tht)_2]$[89] and $(NBu_4)_2[Pt(C{\equiv}CR)_4]$[57] (R = 4-$CH_3C_6H_4$, 4-$CF_3C_6H_4$) were prepared as described previously.

Synthesis of the precursor $(NBu_4)_2[Pt\{C{\equiv}C(1\text{-naphthyl})\}_4]$: This new precursor was synthesized by a similar procedure to that recently reported for the synthesis of related homoleptic derivatives.[57] $[PtCl_2(tht)_2]$ (0.30 g, 0.68 mmol) was added to a fresh solution of LiC≡CNp (4.08 mmol) in diethyl ether at a low temperature (−30 °C). After stirring at a low temperature for 10 min, the mixture was allowed to reach room temperature (ca. 30 min) and the solvent was removed under reduced pressure. The crude residue was treated with deoxygenated *i*PrOH, filtered under argon and the filtrate collected over a solution of NBu_4Br in *i*PrOH (0.55 g, 1.70 mmol) to yield $(NBu_4)_2[Pt(C{\equiv}CNp)_4]$ as a yellow-orange solid, which was filtered, washed with H_2O and air-dried (0.43 g, 50% yield.). ^{1}H NMR (400 MHz, $CDCl_3$, 20 °C): δ = 9.26 (d, J(H,H) = 8.2 Hz, 1H), 7.76 (d, J(H,H) = 8.0 Hz, 1H), 7.70 (d, J(H,H) = 7.1 Hz, 1H), 7.58 (d, J(H,H) = 8.1 Hz, 1H), 7.36 (m, 3H) (Np), 3.55 (m, 16H, N-CH_2-), 1.51 (m, 16H, -CH_2-), 1.32 (m, 16H, -CH_2-), 0.55 ppm (t, 24H, -CH_3) (NBu_4); IR (Nujol): $\tilde{\nu}$ = 2065 cm^{-1} (C≡C); MS (ES+): *m*/*z* (%): no molecular peak was observed; Λ_M(acetonitrile) = 232.1 cm$^2\,\Omega^{-1}$mol^{-1}; elemental analysis calcd (%) for $C_{80}H_{100}N_2Pt$ (1284.77): C 74.79, H 7.84, N 2.18; found: C 74.55, H 7.90, N 2.30.

Synthesis of $[Pt_2Tl_4\{C{\equiv}C(4\text{-}CH_3C_6H_4)\}_8]$ (1): $[PtCl_2(tht)_2]$ (0.40 g, 0.90 mmol) was added to a fresh (−10 °C) solution of LiC≡C(4-$CH_3C_6H_4$) (5.42 mmol) in Et_2O (40 cm^3). The mixture was stirred at this temperature for 5 min and then allowed to reach room temperature (ca. 20 min). The resulting white suspension was evaporated to dryness, and the final oily residue, which contains $Li_2[Pt\{C{\equiv}C(4\text{-}CH_3C_6H_4)\}_4]$, was treated with deoxygenated water (≈20 cm^3). The yellow aqueous solution was rapidly filtered under nitrogen through Celite, and the filtrate treated with a solution of $TlNO_3$ (0.60 g, 2.26 mmol) in H_2O (5 cm^3) to yield $[Pt_2Tl_4\{C{\equiv}C(4\text{-}CH_3C_6H_4)\}_8]$ as a yellow-orange solid, which was filtered and washed with H_2O and air-dried (0.89 g, 92.5% yield). ^{1}H NMR (300 MHz, [D$_6$]acetone, 20 °C): δ = 7.02, 6.94 (AB system, J(H,H) = 7.6 Hz, 4-$CH_3C_6H_4$), 2.30 ppm (s, 4-$CH_3C_6H_4$); ^{13}C{^{1}H} NMR (75.5 MHz, $CDCl_3$, 20 °C): δ = 137.0 (s, C-4), 132.4, 131.0 (s, C-2, C-3), 122.1 (s, C-1) (4-$CH_3C_6H_4$), 117.5 (s, C-α), 109.6 (s, C-β) (C≡C), 21.5 ppm (s, 4-$CH_3C_6H_4$); IR (Nujol): $\tilde{\nu}$ = 2086 cm^{-1} (C≡C); MS(FAB+): *m*/*z* (%): 2333 (35) $[Pt_2Tl_4(C{\equiv}CC_6H_4CH_3)_8 + Tl]^+$, 1269 (60) $[PtTl_3(C{\equiv}CC_6H_4CH_3)_4]^+$; Λ_M = 1.5 cm$^2\,\Omega^{-1}$mol^{-1}; elemental analysis calcd (%) for $C_{36}H_{28}Tl_2Pt$ (1064.45): C 40.62, H 2.65; found: C 40.57, H 2.37.

Synthesis of $[Pt_2Tl_4\{C{\equiv}C(1\text{-naphthyl})\}_8]$ (2):

Method a: Following the procedure described for the synthesis of **1**, the reaction of $Li_2[Pt\{C{\equiv}C(1\text{-naphthyl})\}_4]$, prepared from $[PtCl_2(tht)_2]$ (0.30 g, 0.68 mmol) and LiC≡C(1-naphthyl) (4.08 mmol), and $TlNO_3$ (0.50 g, 1.88 mmol) in *i*PrOH gave **2** as a yellow-orange solid (0.49 g, 60% yield).

Method b: A solution of $(NBu_4)_2[Pt\{C{\equiv}C(1\text{-naphthyl})\}_4]$ (0.15 g, 0.12 mmol) in acetone (20 mL) was treated with $TlPF_6$ (0.081 g, 0.12 mmol) and the mixture stirred for 1.5 h. The resulting yellow-orange solid **2** was filtered and washed with acetone (0.09 g, 80% yield).

Data for 2: ^{1}H NMR (300 MHz, $CDCl_3$, 20 °C): δ = 8.82 (d, J(H,H) = 8.4 Hz, 1H), 7.78 (d, J(H,H) = 8.1 Hz, 1H), 7.66 (d, J(H,H) = 8.2 Hz, 1H), 7.39 (pseudotriplet), J(H,H) ≈ 7.4 Hz, 1H), 7.14 (m, 2H), 6.99 ppm (st, J(H,H) = 8.3 Hz, 1H) (Np); IR (Nujol): $\tilde{\nu}$ = 2079 cm^{-1} (C≡C); elemental analysis calcd (%) for $C_{96}H_{56}Pt_2Tl_4$ (1208.58): C 47.70, H 2.34; found: C 47.52, H 2.28.

Synthesis of $[PtTl_2\{C{\equiv}C(4\text{-}CF_3C_6H_4)\}_4]$ (3): Complex **3** was obtained as a pale yellow solid (1.48 g, 85% yield) in a similar way to complex **1**, but by using $Li_2[Pt\{C{\equiv}C(4\text{-}CF_3C_6H_4)\}_4]$ (1.336 mmol), which was prepared from $[PtCl_2(tht)_2]$ (0.6 g, 1.336 mmol) and LiC≡C(4-$CF_3C_6H_4$) (9.495 mmol). ^{1}H NMR (300 MHz, [D$_6$]acetone, 20 °C): δ = 7.48, 7.42 ppm (AB system, J(H,H) = 8.2 Hz, (4-$CF_3C_6H_4$); ^{13}C{^{1}H} NMR (75.5 MHz, [D$_6$]acetone, 20 °C): δ = 132.6 (s, C-2), 131.0 (s, C-1), 128.3 (q, ^{2}J(C,F) = 32 Hz, C-4), 125.8 (q, ^{3}J(C,F) = 3.7 Hz, C-3) (4-$CF_3C_6H_4$), 125.2 (q, ^{1}J(C,F) = 271 Hz, CF_3), 115.8 (s, C-α, ^{1}J(Pt,C) = 981 Hz), 115.6 ppm (s, C-β, ^{2}J(Pt,C) = 273 Hz) (C≡C); ^{19}F NMR (300 MHz, [D$_6$]acetone, 20 °C): δ = −144.76 ppm (s, CF_3); IR (Nujol): $\tilde{\nu}$ = 2089 cm^{-1} (C≡C); MS (ES+): *m*/*z* (%): 1077 (31) $[PtTl(C{\equiv}CC_6H_4CF_3)_4+H]^+$, 908 (11) $[PtTl(C{\equiv}CC_6H_4CF_3)_3+H]^+$; Λ_M = 15 cm$^2\,\Omega^{-1}$mol^{-1}; elemental analysis calcd (%) for $C_{36}H_{16}F_{12}Tl_2Pt$ (1280.33): C 33.77, H 1.26; found: C 33.73, H 1.15.

X-ray crystallography: Table 5 reports details of the structural analyses for all the complexes. Orange-yellow crystals of **1**·4 acetone were prepared by slow diffusion of acetone into a solution of the compound in tetrahydrofuran, while orange crystals of **2**·3 acetone·$^{1}/_{3}$ H_2O were obtained by direct diffusion of an acetone solution of $TlPF_6$ into an acetone solution of $(NBu_4)_2[Pt(C{\equiv}CNp)_4]$. Yellow crystals of $[PtTl_2(C{\equiv}CTol_F)_4$-(acetone)(dioxane)]$_\infty$ (**3b**) were obtained by slow evaporation of a solution of **3** into a mixture of acetone/dioxane (5:1) at room temperature. For all the complexes, X-ray intensity data were collected with a Nonius KappaCCD area-detector diffractometer using graphite-monochromated $Mo_{K\alpha}$ radiation ($\lambda(Mo_{K\alpha})$ = 0.71071 Å). Images were processed using the DENZO and SCALEPACK suite of programs,[90] and the absorption correction was performed using XABS2[91] (**1**·4 acetone) or SORTAV[92] (**2**·3 acetone·$^{1}/_{3}$ H_2O, **3b**). All the structures were solved by direct methods using the SHELXL-97 program,[93] and were refined by full-matrix least-squares on F^2 with SHELXL-97. All non-hydrogen atoms were assigned anisotropic displacement parameters. The aromatic and methylenic hydrogen atoms were constrained to idealized geometries with isotropic displacement parameters fixed at 1.2 times the U_{iso} value of their attached carbon atoms and at 1.5 times the U_{iso} value for the methyl groups. For complex **3b**, three of the CF_3 groups present positional disorder and could be refined over two positions, with partial occupancy factors of 0.7/0.3 (those corresponding to C9 and C18) and 0.5/0.5 (for C36).

Table 5. Crystallographic data for **1**·4 acetone, **2**·3 acetone·$^1/_3$ H_2O and **3b**.

	1·4 acetone	**2**·3 acetone·$^1/_3$ H_2O	**3b**
empirical formula	$C_{42}H_{40}O_2PtTl_2$	$C_{52.50}H_{37}O_{1.83}PtTl_2$	$C_{43}H_{30}F_{12}O_3PtTl_2$
formula weight	1180.57	1300.98	1426.50
T [K]	173(1)	173(1)	223(1)
crystal system	triclinic	cubic	triclinic
space group	$P\bar{1}$	$Ia\bar{3}d$	$P\bar{1}$
crystal dimensions [mm]	0.20×0.15×0.10	0.20×0.20×0.10	0.30×0.15×0.10
a [Å]	10.5532(2)	38.9950(11)	9.4480(2)
b [Å]	13.3570(2)	38.9950(11)	15.6230(3)
c [Å]	14.5300(3)	38.9950(11)	16.3570(3)
α [°]	70.0140(10)	90	67.9380(10)
β [°]	83.8810(10)	90	85.7680(10)
γ [°]	81.0370(10)	90	77.4550(10)
V [Å^3], Z	1898.14(6), 2	59296(3), 48	2184.10(7), 2
ρ_{calcd} [g cm^{-3}]	2.066	1.749	2.169
μ [mm^{-1}]	12.177	9.365	10.643
θ range [°]	1.96–26.02	2.09–23.25	2.21–27.92
reflections measured	7640	28124	34374
unique reflections, R_{int}	7640, 0.0000	3547, 0.0599	10379, 0.0583
data/restraints/params	7460/0/432	3547/6/156	10379/0/513
goodness of fit on F^2	1.011	1.249	1.014
final R indices [$I>2\sigma(I)$]	$R_1=0.0409$	$R_1=0.0828$	$R_1=0.0479$
	$wR_2=0.0959$	$wR_2=0.1822$	$wR_2=0.0935$
R indices (all data)	$R_1=0.0590$	$R_1=0.1028$	$R_1=0.0964$
	$wR_2=0.1034$	$wR_2=0.1894$	$wR_2=0.1106$
max/min $\Delta\rho$ [e Å^{-3}]	2.137, −1.771	1.124, −1.186	0.994, −1.665

For complex **2**, both of the acetone molecules in the asymmetric unit also showed some disorder and were modelled adequately. For complexes **1** and **2** some residual peaks larger than 1 e Å^{-3} were observed in the vicinity of the heavy atoms (**1**) or in the disorder solvent (**2**), but these had no chemical significance. The low quality of the crystals of **2**·3 acetone·$^1/_3$ H_2O prevented the observation of reflections at high θ values.

CCDC-270168–270170 contain the supplementary crystallographic data for this paper. These data can be obtained free of charge via www.ccdc.cam.ac.uk/data_request/cif.

Acknowledgements

This work was supported by the Spanish Ministry of Science and Technology (Project BQU2002-03997-C02-01,02). B.G. wishes to thank the C.S.I.C. for a grant.

[1] J. M. Lehn, *Supramolecular Chemistry: Concepts and Perspectives*, VCH, Weinheim, **1995**.
[2] S. S. Sun, A. J. Lees, *Coord. Chem. Rev.* **2002**, *230*, 171.
[3] M. Fujita, *Chem. Soc. Rev.* **1998**, *27*, 417, and references therein.
[4] I. Haiduc, F. T. Edelman, *Supramolecular Organometallic Chemistry*, Wiley-VCH, Weinheim, **1999**.
[5] M. A. Casado, J. J. Pérez-Torrente, J. M. López, M. A. Ciriano, F. J. Lahoz, L. A. Oro, *Inorg. Chem.* **1999**, *38*, 2482.
[6] *Extended Linear Chain Compounds* (Ed.: J. S. Miller), Plenum Press, New York, **1982**.
[7] *Inorganic and Organometallic Polymers with Special Properties* (Ed.: R. M. Laine), NATO ASI Series, Kluwer, Dordrecht, **1992**.
[8] J. E. Mark, H. R. Allcock, R. West, *Inorganic Polymers*, Prentice Hall, Englewood Cliffs, NJ, **1992**.
[9] J. K. Bera, K. R. Dunbar, *Angew. Chem.* **2002**, *114*, 4633; *Angew. Chem. Int. Ed.* **2002**, *41*, 4453, and references therein.
[10] L. H. Gade, *Angew. Chem.* **2001**, *113*, 3685; *Angew. Chem. Int. Ed.* **2001**, *40*, 3573, and references therein.
[11] P. Pyykkö, *Chem. Rev.* **1997**, *97*, 597.
[12] A. Burini, J. P. Fackler, Jr., R. Galassi, T. A. Grant, M. A. Omary, M. A. Rawashdeh-Omary, B. R. Pietroni, R. J. Staples, *J. Am. Chem. Soc.* **2000**, *122*, 11264.
[13] K. Sakai, E. Ishigami, Y. Konno, T. Kajiwara, T. Ito, *J. Am. Chem. Soc.* **2002**, *124*, 12088.
[14] I. Ara, J. Forniés, J. Gómez, E. Lalinde, M. T. Moreno, *Organometallics* **2000**, *19*, 3137.
[15] E. J. Fernández, A. Laguna, J. M. López de Luzuriaga, F. Mendizábal, M. Monge, M. E. Olmos, J. Pérez, *Chem. Eur. J.* **2003**, *9*, 456.
[16] M. S. Stender, R. L. White-Morris, M. M. Olmstead, A. L. Balch, *Inorg. Chem.* **2003**, *42*, 4504.
[17] A. F. Heyduk, D. J. Krodel, E. E. Meyer, D. G. Nocera, *Inorg. Chem.* **2002**, *41*, 634.
[18] A. Hayashi, M. M. Olmstead, S. Attar, A. L. Balch, *J. Am. Chem. Soc.* **2002**, *124*, 5791.
[19] W. Y. Wong, G. L. Lu, L. Lin, J. X. Shi, Z. Lin, *Eur. J. Inorg. Chem.* **2004**, 2066.
[20] Y. A. Lee, J. E. McGarrah, R. J. Lachicotte, R. Eisenberg, *J. Am. Chem. Soc.* **2002**, *124*, 10662.
[21] M. E. Prater, L. E. Pence, R. Clérac, G. M. Finniss, C. Campana, P. Auban-Senzier, D. Jérome, E. Canadell, K. R. Dunbar, *J. Am. Chem. Soc.* **1999**, *121*, 8005.
[22] F. A. Cotton, E. V. Dikarev, M. A. Petrukhina, *J. Organomet. Chem.* **2000**, *596*, 130.
[23] F. P. Pruchnik, P. Jakimowicz, Z. Civnik, K. Stanislawek, L. A. Oro, C. Tejel, M. A. Ciriano, *Inorg. Chem. Commun.* **2001**, *4*, 19.
[24] N. L. Coker, J. A. K. Bauer, R. C. Elder, *J. Am. Chem. Soc.* **2004**, *126*, 12.
[25] J. A. Bailey, M. G. Hill, R. E. Marsh, V. M. Miskowski, W. P. Schaefer, H. B. Gray, *Inorg. Chem.* **1995**, *34*, 4591, and references therein.
[26] A. P. Zipp, *Coord. Chem. Rev.* **1998**, *84*, 47.
[27] K. Krogmann, *Angew. Chem.* **1969**, *81*, 10; *Angew. Chem. Int. Ed. Engl.* **1969**, *8*, 35.
[28] V. H. Houlding, V. M. Miskowski, *Coord. Chem. Rev.* **1991**, *111*, 145.
[29] G. A. Crosby, K. R. Kendrick, *Coord. Chem. Rev.* **1998**, *171*, 407.
[30] S. W. Lai, H. W. Lam, W. Lu, K. K. Cheung, C. M. Che, *Organometallics* **2002**, *21*, 226.

[31] H. Gliemann, H. Yersin, *Struct. Bonding (Berlin)* **1985**, *62*, 87.
[32] J. M. Williams, *Adv. Inorg. Chem. Radiochem.* **1983**, *25*, 235.
[33] C. A. Daws, C. L. Exstrom, J. R. Sowa, K. R. Mann, *Chem. Mater.* **1997**, *9*, 363.
[34] C. L. Exstrom, M. K. Pomije, K. R. Mann, *Chem. Mater.* **1998**, *10*, 942.
[35] C. E. Buss, K. R. Mann, *J. Am. Chem. Soc.* **2002**, *124*, 1031.
[36] G. Aullón, S. Alvarez, *Chem. Eur. J.* **1997**, *3*, 655.
[37] M. Dolg, P. Pyykkö, N. Runeberg, *Inorg. Chem.* **1996**, *35*, 7450.
[38] J. Forniés, A. Martin in *Metal Clusters in Chemistry, Vol. 1* (Eds.: P. Braunstein, L. A. Oro, P. R. Raithby), Wiley-VCH, Weinheim, **1999**, p. 417.
[39] J. Forniés, S. Ibañez, A. Martín, B. Gil, E. Lalinde, M. T. Moreno, *Organometallics* **2004**, *23*, 3963.
[40] T. Yamaguchi, F. Yamazaki, T. Ito, *J. Am. Chem. Soc.* **1999**, *121*, 7405.
[41] J. K. Nagle, A. L. Balch, M. M. Olmstead, *J. Am. Chem. Soc.* **1988**, *110*, 319.
[42] A. L. Balch, F. Neve, M. M. Olmstead, *Inorg. Chem.* **1991**, *30*, 3395, and references therein.
[43] S. A. Clodfelter, T. M. Doede, B. A. Brennan, J. K. Nagle, D. P. Bender, W. A. Turner, P. M. Lapunzina, *J. Am. Chem. Soc.* **1994**, *116*, 11379.
[44] V. Zhon, Y. Xu, L. L. Koh, P. H. Leung, T. S. A. Hor, *Inorg. Chem.* **1993**, *32*, 1875.
[45] E. J. Fernández, J. M. López de Luzuriaga, M. Monge, M. E. Olmos, J. Pérez, A. Laguna, *J. Am. Chem. Soc.* **2002**, *124*, 5942.
[46] E. J. Fernández, A. Laguna, J. M. López de Luzuriaga, M. E. Olmos, J. Pérez, *Chem. Commun.* **2003**, 1760.
[47] F. Jalilehvand, L. Eriksson, J. Glaser, M. Maliarik, J. Mink, M. Sandström, I. Tóth, J. Tóth, *Chem. Eur. J.* **2001**, *7*, 2167.
[48] E. G. Mednikov, L. F. Dahl, *Dalton Trans.* **2003**, 3117.
[49] V. J. Catalano, M. A. Malwitz, *J. Am. Chem. Soc.* **2004**, *126*, 6560.
[50] J. R. Stork, M. M. Olmstead, A. L. Balch, *J. Am. Chem. Soc.* **2005**, *127*, 6512.
[51] R. Usón, J. Forniés, M. Tomás, R. Gade, *J. Am. Chem. Soc.* **1995**, *117*, 1837.
[52] G. Ma, A. Fisher, J. Glaser, *Eur. J. Inorg. Chem.* **2001**, 1311.
[53] G. Ma, A. Fisher, J. Glaser, *Eur. J. Inorg. Chem.* **2002**, 1307.
[54] G. Ma, M. Kritikos, M. Maliarik, J. Glaser, *Inorg. Chem.* **2004**, *43*, 4328.
[55] V. J. Catalano, B. L. Bennett, S. Muratidis, B. C. Noll, *J. Am. Chem. Soc.* **2001**, *123*, 173.
[56] O. Renn, B. Lippert, I. Mutikainem, *Inorg. Chim. Acta* **1993**, *208*, 219.
[57] J. Benito, J. R. Berenguer, J. Forniés, B. Gil, J. Gómez, E. Lalinde, *Dalton Trans.* **2003**, 4331.
[58] C. K. Hui, B. W. K. Chu, N. Zhu, V. W. W. Yam, *Inorg. Chem.* **2002**, *41*, 6178.
[59] D. K. C. Tears, D. R. McMillin, *Coord. Chem. Rev.* **2001**, *211*, 195.
[60] W. B. Connick, D. Geiger, R. Eisenberg, *Inorg. Chem.* **1999**, *38*, 3264.
[61] N. Chawdhury, A. Kohler, R. H. Friend, W. Y. Wong, J. Lewis, M. Younus, P. R. Raithby, T. C. Corcoran, M. R. A. Al-Mandhary, M. S. Khan, *J. Chem. Phys.* **1999**, *110*, 4963.
[62] L. Sacksteder, E. Baralt, B. A. Degraff, C. M. Lukehart, J. N. Demas, *Inorg. Chem.* **1991**, *30*, 2468.
[63] V. W. W. Yam, C. K. Hui, S. Y. Yu, N. Zhu, *Inorg. Chem.* **2004**, *43*, 812.
[64] Q.-H. Wei, G.-Q. Yin, Z. Ma, L.-X. Shi, Z.-N. Chen, *Chem. Commun.* **2003**, 2188.
[65] R. Ziessel, M. Hissler, A. El-ghayoury, A. Harriman, *Coord. Chem. Rev.* **1998**, *178–180*, 1251.
[66] V. W. W. Yam, *Acc. Chem. Res.* **2002**, *35*, 555.
[67] I. Ara, J. R. Berenguer, E. Eguizábal, J. Forniés, J. Gómez, E. Lalinde, *J. Organomet. Chem.* **2003**, *670*, 221.
[68] J. Forniés, J. Gómez, E. Lalinde, M. T. Moreno, *Inorg. Chem.* **2001**, *40*, 5415.
[69] J. P. H. Chartman, J. Forniés, J. Gómez, E. Lalinde, R. I. Merino, M. T. Moreno, *Organometallics* **1999**, *18*, 3353.
[70] I. Ara, J. Forniés, J. Gómez, E. Lalinde, R. I. Merino, M. T. Moreno, *Inorg. Chem. Commun.* **1999**, *2*, 62.
[71] J. R. Berenguer, J. Forniés, J. Gómez, E. Lalinde, M. T. Moreno, *Organometallics* **2001**, *20*, 4847, and references therein.
[72] J. P. H. Charmant, J. Forniés, J. Gómez, E. Lalinde, R. I. Merino, M. T. Moreno, A. G. Orpen, *Organometallics* **2003**, *22*, 652.
[73] I. Ara, J. R. Berenguer, J. Forniés, J. Gómez, E. Lalinde, A. Martín, R. I. Merino, *Inorg. Chem.* **1997**, *36*, 6461.
[74] D. Zhang, D. B. McConville, J. M. Hrabusa III, C. A. Tessier, W. J. Youngs, *J. Am. Chem. Soc.* **1998**, *120*, 3506.
[75] W. J. Youngs, C. A. Tessier, J. D. Bradshaw, *Chem. Rev.* **1999**, *99*, 3153.
[76] L. R. Falvello, S. Fernández, J. Forniés, E. Lalinde, F. Martínez, M. T. Moreno, *Organometallics* **1997**, *16*, 1323.
[77] H. Lang, D. S. A. George, G. Rheinwald, *Coord. Chem. Rev.* **2000**, *206–207*, 101.
[78] I. Ara, J. R. Berenguer, E. Eguizábal, J. Forniés, E. Lalinde, *Organometallics* **2001**, *20*, 2686.
[79] L. Hao, J. J. Vittal, R. J. Puddehphatt, *Inorg. Chem.* **1996**, *35*, 269.
[80] C. Janiak, *Coord. Chem. Rev.* **1997**, *163*, 107.
[81] M. Sawamura, H. Iikura, E. Nakamura, *J. Am. Chem. Soc.* **1996**, *118*, 12850.
[82] W. Frank, G. Korrell, G. J. Reiss, *J. Organomet. Chem.* **1996**, *506*, 293.
[83] K. W. Hellmann, C. H. Galka, L. H. Gade, A. Steiner, D. S. Wright, T. Kotte, D. Stalke, *Chem. Commun.* **1998**, 549.
[84] C. H. Galka, L. H. Gade, *Inorg. Chem.* **1999**, *38*, 1038.
[85] At concentrations higher than 2.7×10^{-3} mol L^{-1}, the band at 445 nm does not obey the Beer–Lambert law.
[86] A. L. Balch, F. Neve, M. M. Olmstead, *J. Am. Chem. Soc.* **1991**, *113*, 2995.
[87] In the case of the emission at 590 nm, the decay measurements also fit to two different components (95, 5%), both of them with lifetimes of 12.0 μs.
[88] J. N. G. Demas, A. Crosby, *J. Phys. Chem.* **1971**, *75*, 991.
[89] R. Usón, J. Forniés, F. Martínez, M. Tomás, *J. Chem. Soc. Dalton Trans.* **1980**, 888.
[90] Z. Otwinowski, W. Minor in *Methods in Enzymology, Vol. 276A* (Eds.: C. V. Carter, Jr., R. M. Sweet), Academic Press, New York, **1997**, p. 307.
[91] S. Parkin, B. Moezzi, H. Hope, *J. Appl. Crystallogr.* **1995**, *28*, 53.
[92] R. H. Blessing, *Acta Crystallogr. Sect. A* **1995**, *51*, 33.
[93] G. M. Sheldrick, SHELX-97, a program for the refinement of crystal structures, University of Göttingen (Germany), **1997**.

Received: April 26, 2005
Published online: September 30, 2005

